Engineering Research Express

TOPICAL REVIEW • OPEN ACCESS

Additive manufacturing of high-performance adsorbents for environmental use

To cite this article: Alvin Lim Teik Zheng *et al* 2025 *Eng. Res. Express* **7** 032001

IOP Publishing Eng. Res. Express 7 (2025) 032001 https://doi.org/10.1088/2631-8695/adfacc

Engineering Research Express

OPEN ACCESS

RECEIVED
3 June 2025

REVISED
30 July 2025

ACCEPTED FOR PUBLICATION
12 August 2025

PUBLISHED
26 August 2025

TOPICAL REVIEW

Additive manufacturing of high-performance adsorbents for environmental use

Alvin Lim Teik Zheng[1,2,*], **Ellie Yi Lih Teo**[2], **Omar Faruqi Marzuki**[2], **Lee Feng Koo**[2], **Tze Jin Wong**[2], **Eric Lim Teik Chung**[3] and **Yoshito Andou**[4]

[1] Institute of Ecoscience Borneo, Universiti Putra Malaysia Sarawak, Bintulu 97008, Sarawak, Malaysia
[2] Department of Science and Technology, Faculty of Humanities, Management and Science, Universiti Putra Malaysia Sarawak, Bintulu 97008, Sarawak, Malaysia
[3] Department of Animal Science, Faculty of Agriculture, Universiti Putra Malaysia, Serdang 43400, Malaysia
[4] Graduate School of Life Sciences and Systems Engineering, Kyushu Institute of Technology, Fukuoka 808-0196, Japan
[*] Author to whom any correspondence should be addressed.

E-mail: alvinltz@upm.edu.my

Keywords: 3D printing, additive manufacturing, advanced adsorbents, environmental remediation

Abstract

The emergence of 3D printing (additive manufacturing) has revolutionized the fabrication of advanced adsorbents. This review provides a comprehensive, analytical assessment of 3D-printed adsorbents, critically evaluating their materials, fabrication methodologies, and performance metrics. The materials discussed include polymers, metal–organic frameworks (MOFs), zeolites, biopolymers, carbon-based materials, and hybrid composites, all of which are evaluated in terms of their adsorption efficiency, selectivity, and functionalization strategies. This review also highlights future research directions, including computational modeling-driven design, multi-material printing strategies, and sustainable material innovations. As additive manufacturing technologies progress, their integration with adsorption science presents significant potential to transform environmental and industrial purification systems.

List of abbreviations

3D	Three-dimensional
ABS	Acrylonitrile Butadiene Styrene
AC	Activated Carbon
CFD	Computational Fluid Dynamics
CS	Chitosan
CuHCF	Copper Hexacyanoferrate
CTAB	Cetyltrimethylammonium Bromide
DFT	Density Functional Theory
DIW	Direct Ink Writing
DLP	Digital Light Processing
FDM	Fused Deposition Modeling
FEA	Finite Element Analysis
FGA	Foaming Gelatin Aerogel
GO	Graphene Oxide
MB	Methylene Blue
MO	Methyl Orange

MOFs	Metal–Organic Frameworks
PEI	Polyethylenimine
PFAS	Per- and Polyfluoroalkyl Substances
PLA	Polylactic Acid
PC	Porous Carbon
PVP	Polyvinylpyrrolidone
PVDF	Polyvinylidene Fluoride
SiOC	Silicon Oxycarbide
SLA	Stereolithography
SLS	Selective Laser Sintering
TC	Tetracycline
TPU	Thermoplastic Polyurethane
VOC	Volatile organic compounds
ZIF-8	Zeolitic Imidazolate Framework-8

1. Introduction

The increasing global demand for efficient and sustainable adsorption technologies has driven significant advancements in material science and engineering. Adsorption processes play a crucial role in mitigating environmental and industrial challenges, including water purification, air filtration, gas separation, and pollutant remediation. Conventional adsorbents such as activated carbon (AC) [1–3], zeolites [120] ,silica gels [121], and metal–organic frameworks (MOFs) [122] have been widely deployed due to their high surface area, tunable porosity, and favorable adsorption kinetics. However, these materials often suffer from structural rigidity, limited recyclability, high production costs, and inefficient regeneration, constraining their long-term applicability [4]. Additionally, the lack of precise control over pore architecture and mass transport properties in traditional adsorbents limits their optimization for targeted adsorption applications.

Recent advancements in additive manufacturing (3D printing) have introduced a paradigm shift in the fabrication of functional adsorbents, offering unprecedented control over structural geometry, hierarchical porosity, and material composition. Unlike conventional manufacturing methods that rely on bulk processing and post-synthetic modifications, 3D printing enables the direct fabrication of adsorbents with tailored architectures, thereby enhancing adsorption capacity, selectivity, and transport efficiency [5, 6]. The ability to design and fabricate adsorbents at the microscale and macroscale allows for the precise manipulation of pore structures, adsorption sites, and fluid flow dynamics, which are critical for optimizing performance in real-world applications. Moreover, multi-material printing and post-print functionalization strategies facilitate the integration of high-performance sorbents such as MOFs, carbon-based materials, and biopolymers into complex, multifunctional adsorption systems.

Several recent reviews have explored the intersection of additive manufacturing and environmental applications, yet important gaps remain that warrant a more comprehensive understanding. Jivrakh and co-workers [7] critically assessed 3D-printed adsorbents, membranes, and catalysts for CO_2 capture and conversion, while Yu and co-workers [8] categorized 3D-printed adsorbent materials and printing techniques for separation processes. Another review provided an extensive analysis of printing strategies and rheological considerations for structured adsorbents and catalysts [9], whereas Finny and co-workers [10] highlighted the role of 3D bioprinting in bioremediation applications. Similarly, other systematic reviews focused on advanced 3D-printed geometries for catalysis and adsorption in reforming reactions and CO_2 capture [11], and membrane technologies for wastewater treatment [12]. While these studies have advanced the field by addressing specific materials, applications, or fabrication strategies, they often remain limited to single pollutant classes, lack comprehensive performance benchmarking across material systems, or provide minimal integration of computational modeling and artificial intelligence (AI)-driven design. A comparative summary of previous reviews and the unique contributions of this work is provided in table 1.

This review advances the field by bridging these gaps through a comparative and analytical synthesis of 3D-printed adsorbents across polymers, MOFs, carbons, ceramics, and hybrid materials, with a particular focus on their material–structure–performance relationships in environmental remediation. In addition, it integrates emerging computational design pathways, bioinspired architectures, and AI-enhanced optimization strategies, offering a future-oriented perspective largely absent in prior works. The discussion focuses on fundamental

Table 1. Comparison of this review with previous reviews on 3D-printed adsorbents for environmental applications.

Past review	Scope	Key features	Limitations
[7]	3D-printed adsorbents, membranes, and catalysts for CO_2 capture, separation, and conversion	Critical assessment of 3D-printed sorbents, membranes, and catalysts with an emphasis on printing techniques, binder impacts, and performance trade-offs	Limited focus on pollutant-specific remediation; centered on CO_2-related applications; lacks integration of computational modeling and AI-driven design
[8]	Adsorption materials for separation processes via 3D printing	Detailed classification of 3D printing strategies (SLA, DIW, FDM, laser methods), analysis of rheological properties, and discussion of different adsorbent materials (MOFs, zeolites, carbons, hydrogels)	Primarily focuses on separation processes; lacks systematic pollutant-removal performance evaluation and future-oriented computational or AI-driven design perspectives
[9]	3D-printed structured adsorbents and catalysts for separation and reaction processes	Extensive analysis of printing strategies, rheology, ink design, and industrial scale-up challenges; bridges additive manufacturing with adsorption and catalysis	Predominantly process- and technique-focused; minimal pollutant-specific performance analysis; lacks forward-looking computational and bioinspired design perspectives
[10]	3D bioprinting for bioremediation	Explores bioprinting for microbial support, enzyme immobilization, heavy metal removal, and bioinspired designs; emphasizes sustainability and emerging interdisciplinary approaches	Primarily bioprinting-centric; less focus on comparing traditional 3D-printed adsorbents or multi-material performance benchmarking
[11]	3D-printed materials for catalysis and adsorption (CO_2 capture & reforming reactions)	Reviews addictive manufacturing techniques for catalytic supports, adsorbents, and reforming applications; includes triply periodic minimal surface (TPMS) designs and heat/mass transfer enhancement	Focused on CO_2 and reforming reactions; lacks broad pollutant-remediation performance mapping and AI-driven computational integration
[12]	3D printing for wastewater treatment (membranes & modules)	Perspective on 3D-printed membranes, spacers, biocarriers, sorbents, and catalysts; emphasizes membrane module innovations for water remediation	Primarily module-focused, limited integration of performance-driven pollutant-specific benchmarking or computational design pathways

principles of 3D printing in the fabrication of adsorbents, with emphasis on the influence of material selection, structural configuration, and printing methodologies on adsorption efficiency. The role of emerging additive manufacturing technologies, such as fused deposition modeling (FDM), stereolithography (SLA), digital light processing (DLP), selective laser sintering (SLS), and direct ink writing (DIW), in controlling adsorption properties is critically examined. These insights highlight the transformative potential of additive manufacturing to advance adsorption science, supporting the development of scalable, high-performance adsorbents for environmental and industrial applications.

2. Fundamentals and techniques of 3D-printed adsorbents

3D printed adsorbents represent a new class of materials designed to address the limitations of conventional adsorbents. The key characteristics of 3D printed adsorbents include customizable geometry, hierarchical porosity, and the ability to integrate multiple materials into a single structure [13, 14]. These features enable enhanced adsorption performance, including higher capacity, faster kinetics, and improved selectivity. Commonly used materials include polymers, MOFs, biopolymers, zeolites, and carbon-based materials. For instance, polymers provide flexibility and ease of printing, while MOFs and zeolites offer high surface area and tunable pore sizes. Biopolymers are environmentally friendly, and carbon-based materials exhibit excellent adsorption capacity for organic pollutants and heavy metals. Table 2 summarizes the respective advantages, limitations, typical materials, and key performance indicators of the commonly applied techniques in 3D printing. This consolidated overview provides a practical reference for selecting appropriate 3D printing methods for specific environmental remediation applications.

2.1. Fused deposition modeling (FDM)

FDM is among the most commonly used 3D printing methods due to its operational simplicity, low cost, and wide accessibility [15]. In this technique, thermoplastic filaments such as polylactic acid (PLA) or acrylonitrile butadiene styrene (ABS) are heated and extruded through a nozzle to form objects layer by layer. FDM is especially appealing for fabricating adsorbents because it supports a variety of polymers and enables moderate porosity and mechanical strength in printed structures. However, one limitation of FDM lies in its relatively low resolution, which restricts the production of fine architectural details. Furthermore, the surface area of FDM-printed adsorbents is typically lower than that achieved by other printing techniques, potentially reducing adsorption efficiency. One example involved the fabrication of cylindrical PLA filters using a nozzle of 0.4 mm diameter at 200 °C with a bed temperature of 50 °C. This approach achieved controlled dimensions (1.45 cm diameter, 0.2 cm height) and 40% infill density, allowing internal porosity optimization for improved fluid flow. These scaffolds were subsequently functionalized with graphene oxide (GO) via dip-coating to maintain structural integrity while enhancing surface adsorption capabilities [25].

2.2. Stereolithography (SLA) and digital light processing (DLP)

SLA and DLP are photopolymerization-based 3D printing techniques that cure liquid resins using light sources. While SLA employs a laser to selectively cure the resin, DLP projects entire images layer by layer, enabling faster print speeds [123]. Both techniques are renowned for their high resolution and capacity to produce adsorbents with intricate geometries and high surface areas. These qualities make SLA and DLP particularly suited for applications requiring precise control over porosity and microchannel design. However, their utility is limited by the narrow selection of photopolymer resins, which may lack optimal adsorption properties, and by the time-consuming nature of post-processing steps like washing and UV curing. Figure 1 illustrates the DLP 3D printing workflow, highlighting how controlled photopolymerization allows the fabrication of microchannel monoliths with enhanced resolution and structural precision for adsorption applications [26]. These structures exhibited markedly reduced pressure drops and improved adsorption kinetics when tested with volatile organic compounds such as butane and cyclohexane, outperforming conventional granular and extruded carbon adsorbents. Grigor and co-workers [27] demonstrated that SLA-based DLP printing allows for the creation of complex channel geometries such as serpentine spirals and helices that significantly enhance gas adsorption performance compared to conventional granular AC and extruded monoliths. These printed structures exhibited up to 1600 $m^2\ g^{-1}$ BET surface area and achieved up to 60% higher equilibrium loading of n-butane while maintaining low pressure drop and robust mechanical strength. Importantly, geometrical features like secondary flow-inducing grooves and extended path lengths were shown to improve mass transfer efficiency and prolong breakthrough times, independent of the degree of activation.

Table 2. Comparative summary of major additive manufacturing techniques for 3D-printed adsorbents.

Technique	Advantages	Limitations	Typical materials	Key performance indicators	References
FDM	Simple operation; cost-effective; broad material availability; suitable for multi-material composites	Low resolution (50–200 μm); anisotropic mechanical properties	Thermoplastics (PLA, ABS, PEEK), polymer–composite blends	Layer thickness, infill density, mechanical strength, print speed	[15–17]
DIW	High versatility; can print viscous inks and pastes; enables hybrid and ceramic structures	Ink formulation challenges; limited structural resolution	Ceramics, hydrogels, polymer–ceramic composites	Rheological behavior, dimensional fidelity, porosity	[18, 19]
SLS	No support structures needed; good for complex geometries; high material diversity	Expensive; longer print times; moderate resolution (80–250 μm)	Polymers, ceramics, MOFs, composites	Energy density, layer bonding, porosity, surface roughness	[20, 21]
SLA	High resolution (∼10 μm); smooth surface finish; suitable for fine features	Brittle photopolymers; limited to photosensitive resins; post-curing required	Photosensitive resins, polymer–ceramic slurries	Print resolution, dimensional accuracy, mechanical stability	[22, 23]
DLP	Very high resolution (∼1 μm); faster than SLA; excellent for intricate structures	Limited build volume; restricted material compatibility	Photosensitive polymers, hybrid resins	Light exposure control, polymerization depth, resolution	[24]

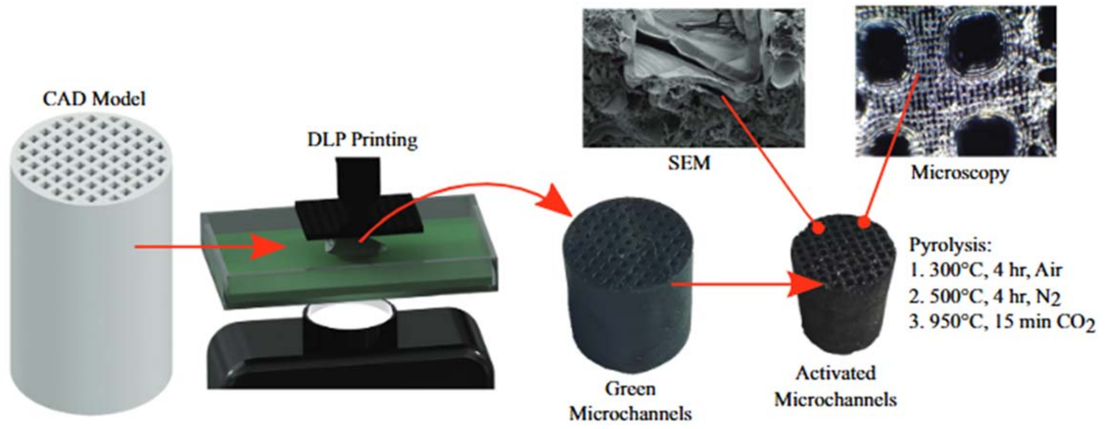

Figure 1. Schematic representation of the DLP 3D printing workflow used to fabricate microchannel monoliths for adsorptive applications [26]. The process involves resin preparation, layer-by-layer photopolymerization using projected light patterns, and post-curing steps to achieve structurally stable monoliths with precisely defined microchannels. This workflow enables the fabrication of complex, high-resolution geometries that enhance mass transfer and surface accessibility for adsorption processes.

2.3. Selective laser sintering (SLS)

SLS is a prominent polymer-based additive manufacturing (AM) technique that employs a high-powered laser to fuse powdered materials, commonly polyamides, layer by layer to form solid structures [28]. This technique is advantageous for creating adsorbents with high mechanical robustness and controlled porosity, and it does not require additional support structures during printing [29]. Nevertheless, SLS tends to be expensive due to the high cost of the laser system and powdered feedstocks. Post-processing, particularly the removal of residual powder, adds further complexity. A representative application involved the fabrication of hybrid membranes composed of chitosan (CS) and thermoplastic polyurethane (TPU). In this method, dry-blended powders were spread into a bed and selectively sintered using a CO_2 laser, which melted TPU to encapsulate CS particles without solvents. This resulted in the creation of superhydrophilic membranes capable of adsorbing Cu (II) and Pb (II) ions at capacities of 19.6 mg g^{-1} and 30.4 mg g^{-1}, respectively. These membranes were further functionalized with Pd for catalytic applications, demonstrating multifunctionality, environmental compatibility, and reusability [30].

2.4. Direct ink writing (DIW)

DIW also referred to as robocasting, is a versatile 3D printing technique that involves extruding a viscoelastic ink to form desired structures. This method accommodates a broad range of material compositions, including functionalized polymers, ceramics, and composites, making it ideal for adsorbent development [31, 32]. The key advantage of DIW lies in its capacity to create tailored macro- and mesoporous architectures with customized surface chemistries. However, the process is highly sensitive to the rheological behavior of the ink, which must be precisely controlled to ensure print fidelity and structural stability [33–35]. Post-printing treatments, such as drying, sintering, or chemical activation, are often required. For instance, DIW was used to produce N-doped porous carbon (PC) monoliths using starch and gelatin as the carbon matrix, melamine as the N source, and SiO_2 microspheres as sacrificial templates. The constructs were printed, freeze-dried, carbonized at 1100 °C, and treated to remove the SiO_2, yielding monoliths with a surface area of up to 816 m^2 g^{-1}. These structures demonstrated rapid dye adsorption, removing 93% of methylene blue (MB) within 10 min, and exhibited durability and reusability over multiple cycles [36].

3. Structural and morphological engineering for enhanced adsorption

3D printing allows for the precise engineering of adsorbent structures at multiple scales. This section explores how lattice design, hierarchical porosity, surface area, and bio-inspired structures can be optimized to enhance adsorption efficiency.

3.1. Lattice design and hierarchical porosity

Lattice engineering and hierarchical porosity are paramount in tailoring mass transfer characteristics and optimizing the accessibility of active sites [37, 38]. These design elements are not merely aesthetic or structural;

they fundamentally reconfigure how fluids interact with the adsorbent material across spatial and temporal scales.

Lattice structures allow for the rational manipulation of surface-to-volume ratio, internal diffusion pathways, and mechanical compliance. Hierarchical structures combine macro-, meso-, and micro-scale features to enhance adsorption [39]. Macro-scale channels improve flow distribution and reduce pressure drop. Meso-scale pores increase accessible surface area and facilitate intermediate diffusion. Micro-scale porosity provides active sites for adsorption and chemical interaction. These multi-scale designs improve mass transfer and accelerate pollutant uptake. They also enhance regeneration performance by improving desorption efficiency. Recent studies have shown that combining these pore types creates adsorbents that perform well under dynamic flow conditions and exhibit improved cycling stability. Printed lattices featuring controlled inter-strut spacing demonstrate improved fluid residence times and reduced concentration polarization, both of which directly influence adsorption kinetics [40]. When these macro-architectures are combined with functional fillers such as MOFs, AC, or doped biochars (BCs), a synergistic effect arises. The structured flow channeling of the lattice enhances mass transport to localized high-affinity regions, thereby maximizing the utility of the embedded adsorbent phase. The study by Wang and co-workers used face-centered cubic (FCC) lattice geometries fabricated via SLA to embed TiO_2 nanoparticles (NPs), thereby optimizing As (III) adsorption performance. Their FCC design maximized surface area while preserving mechanical stability and internal pore connectivity. It was found that TiO_2 NPs retained high adsorption capacities when doped into macrostructures, and that specific geometries (e.g., 2.5 mm lattice grids) allowed repeated regeneration without performance loss [41].

Herein, material extrusion and photopolymerization techniques offer varying degrees of control over porosity [42]. DIW can embed controlled mesoporosity through ink formulation and extrusion patterning, while DLP enables voxel-level precision in macroporous lattice generation. However, the integrity of these structures is strongly influenced by ink rheology, drying shrinkage, and post-processing conditions. Subtle variations in layer resolution or strut diameter can lead to pore occlusion or inconsistent flow behavior, which may impair adsorption repeatability and device robustness. Moreover, the integration of porosity must be evaluated in tandem with mechanical and thermal properties. Overly porous scaffolds may exhibit increased surface area but suffer from mechanical collapse or fragmentation under flow.

3.2. Role of surface area and pore interconnectivity

The efficiency of 3D-printed adsorbents is primarily determined by the balance between their accessible surface area and the degree of pore network connectivity. These structural parameters control not only the quantity of available adsorption sites but also the rate and efficiency of mass transfer, which are particularly critical in continuous flow or high-load scenarios [43]. The mere presence of porosity is insufficient; it is the spatial arrangement, connectivity, and accessibility of these pores that determine how effectively adsorbates interact with the internal surface of the adsorbent.

Surface area enhancement alone, as seen in powdered adsorbents or high-surface-area nanomaterials, does not guarantee efficient pollutant removal when mass transfer is hindered by tortuous or isolated pore structures [44]. In contrast, 3D-printed architectures allow for deliberate design of interconnected pores, enabling more uniform distribution of flow and minimizing dead zones. This design approach ensures that the entire internal surface contributes to adsorption, rather than confining interactions to the external layer or select pore networks. The advantage of engineered pore interconnectivity has been demonstrated in various material systems. A recent study exemplifies the critical balance between surface area preservation and interfacial tuning in composite sorbents [45]. Using DIW, they fabricated lattice monoliths comprising foaming gelatin aerogel (FGA) and PC, yielding surface areas exceeding 1000 $m^2\ g^{-1}$. Notably, despite partial pore obstruction by the aerogel matrix, the composites retained accessible mesoporous domains and demonstrated remarkable selectivity for anionic dyes, with removal efficiencies reaching 99% for Orange-G. This selectivity was not merely a function of surface area, but stemmed from charge redistribution at the FGA–PC interface, as confirmed by XPS and density functional theory (DFT) simulations. These findings reinforce that surface accessibility must be coupled with functionalized pore surfaces and interfacial electrostatics to achieve discriminative adsorption, particularly in multicomponent pollutant systems.

Moreover, the pore interconnectivity of 3D-printed materials enables dynamic adsorption behavior, such as faster breakthrough times and reduced pressure drops in fixed-bed operations. This is especially relevant when designing for turbulent or transitional flow regimes, where adsorbents must withstand both mechanical stress and performance consistency [46]. Zhu and colleagues demonstrated that pore interconnectivity plays a decisive role in fixed-bed adsorption systems, where fluid dynamics and continuous pollutant loading impose operational constraints that surface area alone cannot resolve. Their 3D-printed AC/alumina monolith, engineered via DIW followed by freeze-drying, exhibited a hierarchically porous framework comprising

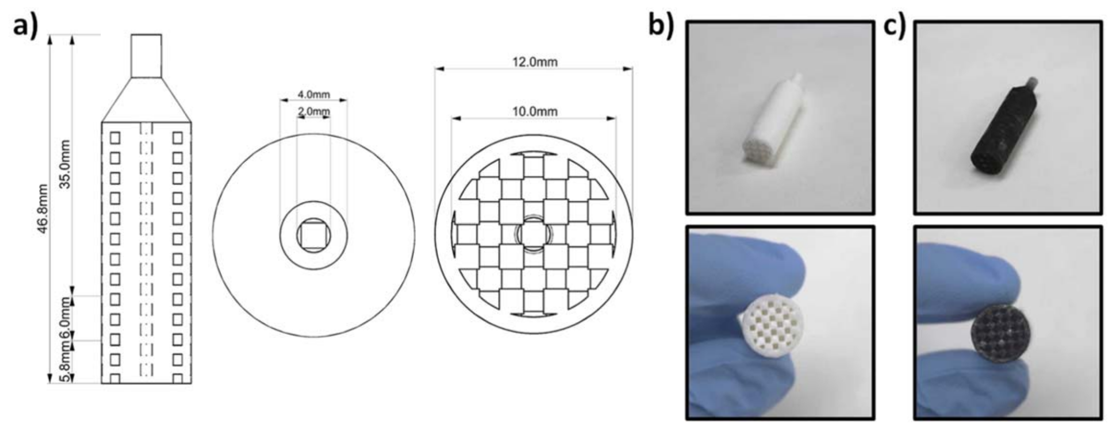

Figure 2. (a) Dimensional specifications of the 3D-printed column design; (b) photograph of the unmodified 3D-printed column; (c) image of the column after *in situ* growth of ZIF-8, forming the c-ZIF-8@3D-printed structure [50]. This modification integrates a high-surface-area metal–organic framework (ZIF-8) onto the 3D-printed scaffold, enhancing its adsorption capacity and selectivity.

interconnected nano-, micro-, and millimeter-scale pores. This architecture established well-aligned adsorption microchannels that significantly reduced mass transfer resistance. In fixed-bed desulfurization of hydrogenated diesel, the monolith achieved 96.6% sulfur removal efficiency, outperforming conventional packed beds with loose particles. The enhanced performance was attributed to the uninterrupted pore networks that enabled rapid internal diffusion and sustained active site accessibility throughout the adsorption cycle [47].

3.3. Bio-inspired and computationally optimized structures

Natural organisms offer design blueprints characterized by high surface-to-volume ratios, interconnected channels, and energy-efficient flow pathways. Bio-inspired design draws on natural structures such as lotus leaves, diatoms, and trabecular bone. These biological models guide the creation of 3D-printed adsorbents with hierarchical porosity, optimized fluid flow pathways, and enhanced mechanical stability. When combined with computational optimization techniques such as topology optimization and generative design, these architectures achieve superior pollutant adsorption performance under diverse flow and pressure conditions.

The layer-by-layer immobilization of CuHCF on 3D-printed PLA scaffolds, as presented previously draws parallels to natural ion-channel architectures, enabling targeted ammonium recovery through engineered selectivity and structural robustness [48]. Computationally guided surface functionalization, such as targeted carboxylation to facilitate copper coordination, demonstrates how biomimetic principles and digital design strategies can be integrated to achieve high functional selectivity in 3D-printed adsorbents. One previous study developed PDA-functionalized MOF/MXene monolithic adsorbents using DLP printing, emulating biological binding environments through surface engineering [49]. Their composite structure exhibited a bioinspired interaction network incorporating electrostatic forces and π–π stacking, while the DLP process enabled precise architectural control of pore connectivity and scaffold rigidity. This illustrates how biomimetic surface chemistry and digitally optimized geometry can jointly advance the design of high-performance adsorbents.

Bauza and colleagues designed a stereolithographically printed cube-array structure coated with ZIF-8-derived PC, forming a hierarchical adsorbent system optimized for continuous-flow extraction [50]. As shown in figure 2, ZIF-8 can be grown *in situ* within a 3D-printed column, producing a c-ZIF-8@3D-printed composite with improved surface area and selective adsorption performance. The cube-array is fabricated into a robust column format suitable for flow-through extraction of pollutants. Using an *in situ* growth method, ZIF-8 was directly deposited onto the 3D-printed device, resulting in a stable and durable integration of the MOF. Column structures composed of interlinked cubes were designed and produced via stereolithography 3D printing using Rigid 10K resin (figure 2(a)). Following the same procedure used for c-ZIF-8@3D-printed cubes, the resulting columns showed a uniform distribution of PC throughout the entire structure (figures 2(b),(c)) [50].The integrated meso- and microporous structure enhanced pollutant access, while the geometrically engineered column format mimicked efficient biological transport channels. The high extraction efficiency for multiple parabens over ten reuse cycles demonstrates the utility of structural optimization in translating material reactivity into functional flow-through architectures.

Computational optimization frameworks, including topology optimization, generative algorithms, and machine learning-based design, are increasingly used in the development of 3D-printed adsorbents. These approaches provide precise control over pore geometry, improve mechanical stability, and optimize flow dynamics. They also enable predictive modeling of adsorption behavior under varying operating conditions, reducing experimental costs and accelerating design iterations. Design tools such as finite element analysis (FEA) and topology optimization can pre-screen geometries based on stress distribution, pressure drop, or contact time, reducing the trial-and-error iterations commonly required in experimental workflows [47, 51]. This shift from empirical prototyping to model-informed fabrication is particularly impactful for flow-based systems, where structural asymmetries or bottlenecks can significantly influence breakthrough behavior.

Jin and co-workers demonstrated that computational modeling, particularly deep learning, can effectively guide the functional design of cetyltrimethylammonium bromide (CTAB)-modified geopolymer adsorbents for tetracycline (TC) removal [52]. Their predictive model accurately captured the pH-dependent adsorption behavior, allowing reliable forecasting of performance under realistic environmental conditions. This integration of structural engineering with AI-based optimization represents a shift toward predictive adsorbent design, where material behavior can be anticipated prior to synthesis.

The combination of biomimicry and machine-driven design allows for the creation of multifunctional adsorbents that integrate pollutant capture with flow regulation, mechanical compliance, or catalytic enhancement. In this context, the adsorbent becomes a dynamic component of the treatment system, rather than a static substrate. The application of generative design algorithms to reproduce bioinspired pore architectures not only increases adsorption surface area but also improves internal fluid dynamics, enabling the entire structure to participate actively in remediation processes. Importantly, these advanced designs are not restricted to aesthetic novelty. Their implementation results in quantifiable improvements in mass transfer efficiency, regeneration ease, and structural durability. As environmental treatment technologies increasingly demand higher throughput, lower energy consumption, and modular integration, the role of computationally optimized, bioinspired architectures will become even more central to the engineering of next-generation adsorbents.

4. Material innovations in 3D printed adsorbents

This section explores the key material innovations in 3D printed adsorbents, including polymer-based materials, MOFs, zeolites, biopolymers, carbon-based materials, and hybrid composites.

4.1. Polymer-based adsorbents

In adsorbent fabrication, polymers such as polylactic acid (PLA), polyvinyl alcohol (PVA), and polyamide (nylon) are frequently used. Previously, a review highlighted recent developments in 3D-printed polymeric structures applied in membrane systems, adsorption, advanced oxidation, bioreactors, and microfluidics [53]. These materials can be functionalized with chemical groups to enhance their adsorption properties. A notable development in polymer-based 3D adsorbents involves thiol–yne photoresins fabricated via SLA using a simple BA/PETMP formulation [54]. These resins enabled the fabrication of intricate architectures with excellent malachite green (MG) dye adsorption performance, achieving >95% removal within 5 min and >90% over 10 reuse cycles. The resin's low swelling in aqueous media (<0.5%) and stable curing without photoblockers highlight its practical scalability. Functional group tuning demonstrated that the presence of surface thiol and hydroxyl moieties critically influenced adsorption kinetics, suggesting synergistic H-bonding and electrostatic interactions.

In addition, increasing infill density enhances mechanical stability but can restrict flow paths, reduce mass transfer rates, whereas introduce gyroid or lattice infill geometries improves fluid distribution and reduces diffusion resistance, thereby accelerating adsorption kinetics. The printing resolution achievable with DIW and SLA also plays a critical role in controlling pore size and surface roughness. Higher resolution printing enables the fabrication of microchannels with improved surface accessibility, as demonstrated by Chaix and co-workers [55], where SLA-printed trianglamine hydrogels exhibited enhanced PFAS adsorption due to optimized channel connectivity.

Geopolymer-based adsorbents have also attracted growing interest in environmental remediation due to their structural tunability, cost-effective raw materials (e.g., metakaolin, fly ash), and high thermal and chemical stability [56–58]. Recent research has shown that incorporating surfactants such as cetyltrimethylammonium bromide (CTAB) into the geopolymer matrix before extrusion facilitates simultaneous surface functionalization, pore structure modulation, and control over surface charge characteristics. A 3D-printed CTAB-geopolymer adsorbent prepared using DIW has shown excellent capability towards absorption of antibiotics [52]. The printed structure exhibited a tailored macroporous framework with interconnected channels and optimized surface charge distribution for the rapid capture of TC under dynamic pH conditions. The positively charged CTA^+ groups in the geopolymer scaffold selectively interacted with anionic TC species, while the macro–micro pore integration facilitated rapid diffusion and uptake [52]. Despite the inherent alkali release of geopolymers, the printed scaffold retained over 84% adsorption efficiency within 302 min and showed promising reusability over multiple cycles.

4.2. Biopolymer

Biopolymers are renewable and biodegradable, making them suitable for environmentally sensitive applications. Advances in tuning ink viscosity and flow behavior have enabled improved layer resolution and printing precision [59, 60]. Biopolymers, such as cellulose [61, 62], CS [63, 64] and alginate [65–67], are gaining attention as sustainable alternatives to synthetic polymers for 3D printing. These materials are derived from natural sources and are biodegradable, making them environmentally friendly. For instance, the incorporation of 3% (w/w) cellulose nanocrystals (CNCs) into PLA matrices via FDM significantly improved mechanical properties (Young's modulus increased ∼30%) and surface wettability (contact angle reduced ∼17%), highlighting the compatibility and interfacial adhesion between CNC and PLA [68].

Central to this advancement is the rheological tunability of biopolymer inks, which governs print fidelity, layer adhesion, and resolution of the final construct. For example, nanocellulose exhibits key viscoelastic properties such as shear thinning, thixotropy, and gelation, which are essential for preserving structural integrity during extrusion-based printing, particularly in liquid deposition modeling (LDM). When functionalized with zero-valent iron (Fe^0) NPs, nanocellulose scaffolds not only exhibit enhanced surface activity but also gain catalytic regeneration potential via *in situ* Fenton-like oxidation [69]. This dual capability transforms printed scaffolds into multifunctional platforms capable of simultaneous pollutant adsorption and degradation, while retaining mechanical and chemical stability across multiple cycles.

4.3. Zeolites

Zeolites remain widely used in adsorption applications due to their well-defined microporous structure and high ion-exchange capacity. Embedding zeolites into 3D-printed architectures has allowed the conversion of conventional granular or powdered forms into structured adsorbents with enhanced mechanical stability, ease of handling, and reusability. Recent studies have highlighted that thermal post-processing, particularly the choice of sintering temperature, plays a critical role in influencing both the structural integrity and adsorption efficiency of 3D-printed zeolite materials. A study examining the thermal behavior of natural zeolite-based prints revealed that sintering at moderate temperatures (e.g., 600 °C) resulted in monoliths with high porosity and preserved crystallinity, leading to superior adsorption of MB. The sample sintered at 600 °C achieved a removal efficiency exceeding 82%, which was significantly higher than that of those sintered at higher temperatures, such as 900 °C, where a loss of crystallinity and porosity diminished adsorption to just 20%. Mechanical strength increased with sintering temperature, yet a trade-off emerged: higher temperatures enhanced compressive modulus but compromised active surface area through pore collapse [70].

The utilization of DIW to fabricate zeolite-Y-based monoliths offers a scalable platform for metal ion remediation in continuous flow systems [71]. Through the integration of nanoclay, PVA, and hydroxyethyl cellulose, the researchers achieved printable pastes with desirable viscoelasticity, leading to robust hyperboloid structures. After calcination, the resultant 3D printed adsorbent displayed a BET surface area of 384 $m^2 g^{-1}$ and efficient removal of Pb^{2+} and Cu^{2+} (>90%) at optimized pH and low flow rates. The adsorption followed pseudo-second-order kinetics, with higher selectivity for Pb^{2+}, attributed to its lower hydrated radius and higher electronegativity. Importantly, the monoliths retained structural integrity and adsorption efficacy over 10 regeneration cycles, emphasizing the mechanical resilience and reusability of these printed adsorbents for industrial-scale water purification. The combination of zeolite with biodegradable PLA to create 3D-printable composites also highlights the promise of hybrid structures for selective adsorption of ammonia [72]. By embedding up to 32% zeolite in PLA matrices, the study achieved spatially customizable and mechanically stable adsorbent disks with consistent ammonia removal under static and dynamic bioassay conditions. These structures not only avoided particle shedding and associated toxicity but also retained functionality in complex media such as sediment elutriates. The selective reduction of ammonia without affecting metal or PAH levels demonstrated the precision of the hybrid system in mitigating toxicity while preserving the integrity of co-existing contaminants.

4.4. Metal–organic frameworks (MOFs)

MOFs are a class of porous materials composed of metal ions coordinated with organic ligands. MOFs are highly attractive for adsorption applications due to their exceptionally high surface area, tunable pore sizes, and chemical functionality [73–75]. Previously, Molavi and co-workers systematically reviewed on 3D printed MOF monolith which covers their synthesis strategies and applications towards environmental remediation [76]. Among the MOFs, Prussian blue analogues (PBAs), particularly copper hexacyanoferrate (CuHCF), have recently demonstrated exceptional selectivity toward ammonium ions, even in the presence of competing cations such as Na^+ and K^+. Recent developments using 3D-printed scaffolds functionalized with carboxyl groups have enabled layer-by-layer immobilization of CuHCF, enhancing both crystallinity and adsorption efficiency [48]. Such integration expands the applicability of MOFs beyond conventional heavy metal removal to targeted nutrient recovery from wastewater.

MOFs like ZIF-8 have also been utilized as sacrificial templates to generate PC layers via carbonization, producing sorbents with enhanced chemical and thermal stability compared to their crystalline counterparts [77]. A notable development involves the *in situ* growth and subsequent pyrolysis of ZIF-8 on stereolithographically printed polymer frameworks to yield a carbon-coated monolith suitable for continuous-flow water treatment. This technique enables the formation of a dual-porous architecture (micro- and mesopores), with enhanced π-π interactions between the carbon surface and organic pollutants such as parabens. The resulting 3D-printed carbon@ZIF-8 devices have shown high removal efficiencies (up to ~96%) for a range of alkylparaben compounds, with stable performance over multiple reuse cycles. In addition to high surface affinity, these systems exhibit impressive mechanical and chemical durability, remaining effective under varied pH and ionic conditions, and even after thermal regeneration. This integration of MOF-derived porosity with geometric precision via 3D printing paves the way for next-generation fixed-bed devices capable of continuous contaminant capture in real-world scenarios, including complex aqueous matrices [50].

Sulfonic-functionalized MIL-100-Fe (MIL-100-Fe-AMSA) presents a notable advancement in MOF-based adsorbents, particularly when incorporated into a 3D-printed solid-phase extraction device [78]. Synthesized via a rapid microwave-assisted method, MIL-100-Fe-AMSA exhibited an exceptionally high adsorption capacity for diclofenac (476 mg g^{-1}), outperforming its unmodified counterpart (357 mg g^{-1}). The enhanced performance was attributed to synergistic π–π interactions and hydrogen bonding between the sulfonic groups and the drug molecules, while adsorption kinetics conformed to a pseudo-second-order model with rapid equilibrium (<5 min). The MOF was further immobilized into a stereolithographically printed column using PVDF ink, enabling simultaneous preconcentration of diclofenac and ketoprofen with enrichment factors of 17 and 9, respectively.

4.5. Carbon-based adsorbents

Carbon-based materials have been fundamental to adsorption science owing to their high surface area, adjustable surface chemistry, and adaptable structural properties [79–82]. In the context of 3D printing, these materials are undergoing a functional transformation from powdered adsorbents to structurally engineered monoliths capable of addressing emerging environmental challenges such as microplastics, nanoplastics, and persistent organic pollutants. Previous reviews have systematically covered on research advances of 3D printing of graphene-based materials for various applications [83, 84].

GO for instance, illustrates the potential and limitations of carbon nanomaterials. While GO offers a high surface area and abundant oxygen-containing functional groups, its tendency to agglomerate in aqueous media limits dispersion and accessibility of active sites [85]. Hybridization with biopolymers such as CS addresses this constraint by combining electrostatic interaction from CS's amino groups with π–π stacking from GO. When this hybrid was grafted onto a 3D-printed silicon oxycarbide (SiOC) scaffold using a silane coupling agent (GLYMO), the resulting composite demonstrated notable structural adhesion and functional retention over five regeneration cycles. It achieved a methyl orange (MO) uptake of 182.25 mg g^{-1} at pH 3 and maintained over 92% efficiency after reuse [86].

AC remains a benchmark material in environmental remediation, but its particulate nature often hinders recovery, reuse, and integration into dynamic systems. The adaptation of AC into printable scaffolds addresses these limitations by embedding powdered AC into robust polymer matrices. Kim and co-workers exemplified this by incorporating powdered AC with polyvinylidene fluoride (PVDF), polyvinylpyrrolidone (PVP), and polyethylenimine (PEI) to create mesoporous monoliths via DIW. These structures exhibited a surface area of 371.3 m^2 g^{-1} and achieved effective adsorption of various nano plastics, including polystyrene (PS) and polyethylene terephthalate (PET), with a maximum capacity of 3.69 mg g^{-1}. The matrix polymers contributed not only mechanical support but also introduced secondary interactions such as electrostatic attraction and hydrogen bonding, enhancing the overall adsorption kinetics and selectivity. Importantly, the printed scaffolds retained structural integrity under flow conditions, overcoming a key limitation of loose AC particles [87].

While carbon-based materials are often derived from refined precursors, BC offers a renewable and increasingly tunable alternative derived from waste biomass [88, 89]. The shift toward BC reflects a broader trend toward circular material engineering, where waste streams are valorized into high-performance environmental technologies. One of the primary challenges in printing BC-based structures lies in preserving its active surface area during ink formulation and post-processing. The use of polymeric binders, while necessary for print fidelity, can occlude functional sites. This issue has been addressed through the inclusion of sacrificial porogens such as calcium carbonate ($CaCO_3$), which are later removed to generate macropores and restore surface accessibility. One previous study demonstrated that rice husk-derived, N-doped BC printed with $CaCO_3$ achieved surface areas up to 1583 m^2 g^{-1} [90]. These monoliths functioned dually as adsorbents and impellers within reactor systems, enabling simultaneous mixing and adsorption, and offering a performance advantage over conventional packed beds. CFD simulations validated that the engineered porosity reduced concentration polarization and enhanced mass transfer, affirming the importance of architectural optimization in performance enhancement. Carbon-based 3D-printed adsorbents embody the integration of structural precision with functional versatility. Additive manufacturing facilitates their conversion into architected monoliths, allowing precise control over pore architecture, enhanced reusability, and seamless integration into engineered systems.

4.6. Metal oxide

Metal oxides have emerged as promising candidates for adsorbent fabrication in 3D printing, particularly in applications where chemical robustness, thermal resistance, and specific surface reactivity are required. Unlike organic polymers or biopolymers, metal oxides can tolerate harsh environmental conditions and maintain structural fidelity under high-temperature operations, making them well-suited for persistent contaminant removal [91–93]. Recent advances demonstrate that 3D printing enables the geometric and surface optimization of metal oxide monoliths, which are otherwise challenging to implement in continuous flow systems due to their brittleness and powdery morphology [94]. Martins and co-workers fabricated extrusion-printed indium oxide (In_2O_3) monoliths with tunable porosity and geometry, designed for the adsorption of perfluorooctanoic acid (PFOA). The adsorption efficiency reached up to 75% within 3 h, with performance enhanced after thermal regeneration at 500 °C. These monoliths exhibited stable performance and mechanical integrity across regeneration cycles. The key functional strength of In_2O_3 in this context lies in its surface oxygen vacancies and Lewis acidity, which promote strong binding with electron-rich moieties in per- and polyfluoroalkyl substances (PFAS) [95]. Unlike conventional adsorbents relying on surface area alone, metal oxides engage in chemisorptive interactions that are more resistant to desorption and fouling [96]. This interaction mode provides a distinct advantage in capturing low-concentration contaminants in complex matrices. Despite their promise, metal oxide-based 3D printed adsorbents remain relatively underexplored.

4.7. Hybrid and composite materials

The development of hybrid and composite adsorbents has become increasingly pivotal in overcoming the intrinsic limitations of single-material systems [97]. Hybrid and multi-material adsorbents combine the functional advantages of polymers, bio-based matrices, and inorganic fillers (e.g., MOFs, carbon nanostructures, metal oxides), creating composites with improved adsorption efficiency and structural integrity. The effectiveness of these materials depends not only on their composition but also on how 3D printing parameters control their microarchitecture and interfacial compatibility. Although materials such as polymers, biopolymers, MOFs, zeolites, and carbon each offer advantageous properties for 3D printing, their use in isolation often entails compromises among printability, mechanical strength, and adsorption efficiency. 3D printing of such composites enables hierarchical designs where each component plays a strategic role.

One previous study demonstrated this synergy in a Cr-MOF@clay composite printed via DLP, achieving a remarkably high specific surface area (4959 m^2 g^{-1}) and efficient removal of MO and direct red 31 at mildly acidic conditions [98]. The MOFs provide high surface area and active sites, while clays contribute structural integrity and modulate mass transport. The introduction of CS as a biopolymeric binder contributed additional amino and hydroxyl functionalities, promoting electrostatic attraction and hydrogen bonding.

Porosity control is also crucial in hybrid systems, particularly when incorporating high-surface-area fillers like MOFs or activated carbons. One representative study reported on the development a binder-free, one-pot 3D printing method to fabricate cellulose-ZIF-8 (CelloZIF-8) composites using TEMPO-oxidized cellulose nanofibrils (TOCNF) mixed with either ZnO precursors or 2-methylimidazole (Hmim) to form printable gels [99]. As illustrated in figure 3, the one-pot printing process allows for the simultaneous fabrication and functionalization of cellulose-based scaffolds with improved adsorption capacity and structural integrity. These inks were printed into porous structures using a standard 3D printer and subsequently soaked in complementary ZIF-8 precursor solutions to induce *in situ* crystal growth. This process produced mechanically stable, highly porous scaffolds with a high ZIF-8 loading (67.5 wt%) without requiring any polymer binders or post-treatment, enabling efficient CO_2 adsorption, dye removal, and heavy metal ion capture. Controlling the ratio of open macropores for flow distribution and micropores for adsorption sites is key to achieving high mass transfer rates and long-term operational stability.

Integrating MOFs with complementary nanomaterials has emerged as an effective strategy to address inherent drawbacks such as limited water stability and particle aggregation. One promising approach involves the *in situ* growth of bimetallic MOFs, such as ZIF-67/ZIF-8, on MXene substrates to produce dense yet

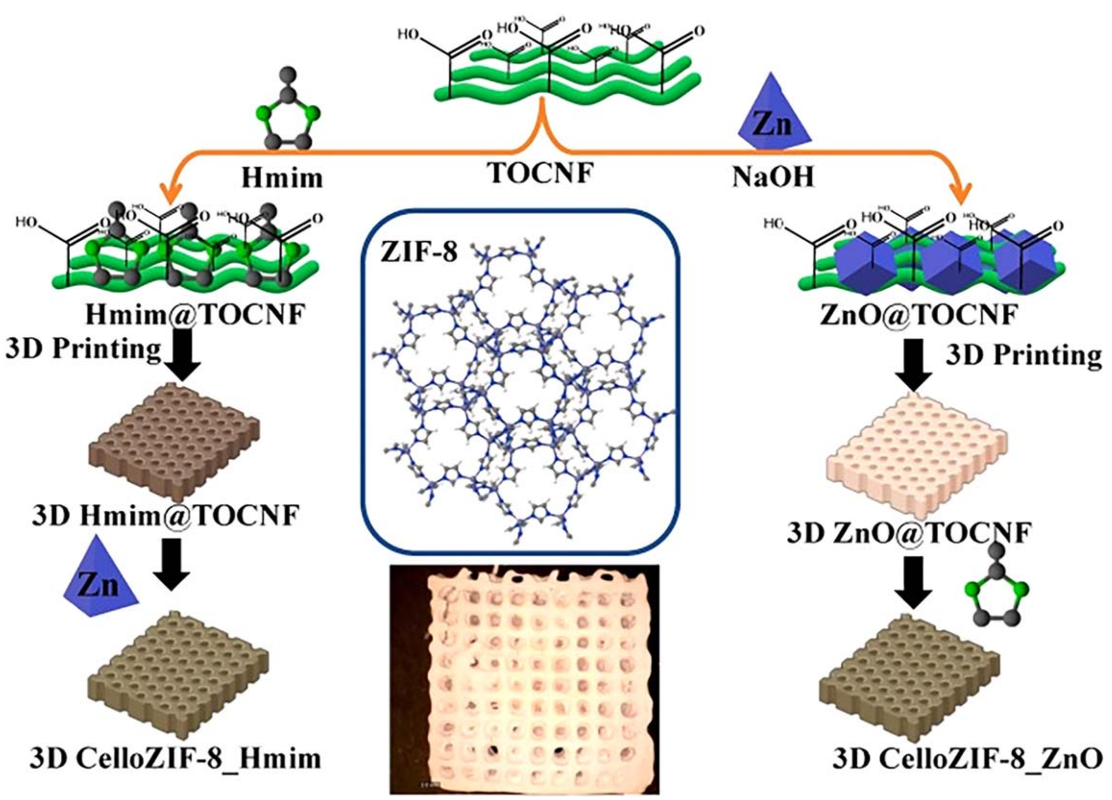

Figure 3. Schematic illustration of the one-pot 3D printing process used to fabricate CelloZIF-8 [99]. This approach combines cellulose-based bio-inks with *in situ* ZIF-8 synthesis during the printing process, resulting in a composite with enhanced mechanical stability and high surface area. The integration of ZIF-8 into the cellulose matrix improves adsorption performance and broadens the applicability of the 3D-printed adsorbent for water treatment.

accessible multilayered composites. Although both MOFs and MXenes offer high surface areas and abundant active sites, their conventional powder forms pose practical challenges for recovery and reuse, highlighting the need for structured or immobilized configurations in real-world applications. One recent work has introduced the concept of immobilizing MOFs/MXene composites onto 3D-printed resin structures using a bioinspired polydopamine (PDA) coating layer [49]. This strategy not only improves the mechanical integrity and reusability of the hybrid adsorbent but also enhances its chemical affinity for pollutants such as dyes and heavy metals. The PDA/MOFs/MXene-coated monoliths demonstrated selective adsorption toward Congo red and Hg^{2+}, achieving removal efficiencies exceeding 99% and 94%, respectively. Notably, the adsorption followed pseudo-second-order kinetics and monolayer Langmuir behavior, indicating chemisorption dominated by π–π stacking, electrostatic interactions, and metal–ligand coordination.

The significance of hybrid composites lies not only in their chemical complexity but also in their adaptability across diverse environmental conditions. In systems where single-material sorbents fail due to structural collapse or surface fouling, composites provide stability and resilience through redundancy in functionality. Moreover, hybridization can facilitate targeted adsorption of structurally diverse contaminants. For instance, π–π stacking, cation–π interactions, and van der Waals forces can be simultaneously leveraged in properly engineered materials to address multicomponent wastewater streams. However, hybrid systems present nontrivial fabrication challenges. Achieving homogeneous dispersion, interfacial compatibility, and printability across components often requires extensive rheological tuning and surface modification.

5. Applications of 3D-printed adsorbents in water purification and wastewater treatment

In this context, 3D-printed adsorbents have emerged not merely as architectural novelties but as functionally engineered platforms that offer programmable porosity, enhanced mass transfer, and pollutant-specific surface functionality [100, 101]. As mentioned, the key advantage of 3D-printed adsorbents lies in their hierarchical pore networks, which optimize both surface accessibility and fluid transport. 3D-printed adsorbents present unique advantages for diverse application scenarios, including heavy metal removal from contaminated water, volatile organic compound (VOC) adsorption, and gas separation in industrial processes. Unlike conventional granular or membrane-like adsorbents, 3D-printed structures can be customized into modular designs, facilitating seamless integration into existing treatment equipment. This modularity reduces retrofitting costs and enhances operational flexibility. Furthermore, additive manufacturing enables hierarchical porosity and tailored surface chemistries, which improve adsorption capacity and selectivity for target pollutants.

A key factor underlying the performance of 3D-printed adsorbents is the interplay between printing parameters and structural properties, which directly affects mass transfer, adsorption kinetics, and cycle stability. For instance, high-precision SLA enables the fabrication of complex gyroid and lattice structures with interconnected pores that enhance convective flow and reduce diffusion resistance. This design was evident in the trianglamine-based hydrogels by Chaix and co-workers [55] which achieved rapid PFAS removal through improved solvent accessibility and uniform charge distribution. For heavy metal remediation, structures functionalized with chelating agents or ion-exchange groups have demonstrated pronounced affinity for Pb^{2+}, Cd^{2+}, and Hg^{2+} ion [102, 103]. Modular inserts or barrier-type configurations printed from metal oxides or polymer–chelator composites can be engineered to capture toxic species such as As and Cr (VI) under dynamic and chemically aggressive flow conditions [104]. The ability to precisely control pore architecture and surface chemistry allows for tailoring adsorbent response to specific ionic radii, oxidation states, or competing ion profiles, parameters that are critical in high ionic strength environments.

Although numerous studies have demonstrated the potential of 3D-printed adsorbents for pollutant removal, direct comparisons are challenging due to variations in experimental conditions, including pH, flow rate, pollutant type, and initial concentrations. Table 3 demonstrates the versatility of 3D-printed adsorbents across a wide range of contaminants, including heavy metals, dyes, volatile organic compounds (VOCs), PFAS, halides, and radionuclides, allowing for a more meaningful evaluation of performance. Among the evaluated materials, GO-based hydrogels and composites consistently delivered high capacities for metal ions such as Cu^{2+} reporting values ranging from 250 $mg\,g^{-1}$ to 633.2 $mg\,g^{-1}$ [101, 111]. These values are significantly higher than those observed in GO-coated polymer scaffolds, indicating that the hydrogel network and surface functionalization strongly influence ion exchange and complexation behavior. For dyes, aerogel-carbon composites and SiOC-GO hybrids performed effectively, achieving removals above 90 percent at moderate concentrations, achieving near-complete removal of Orange G [45] and MO [86]. These results highlighted the role of hierarchical porosity and hydrophilic functional groups in enhancing diffusion and electrostatic interactions with dye molecules. Similarly, one study reported that hierarchical carbonaceous films removed formaldehyde with cumulative dynamic capacities of 241.7 $mg\,g^{-1}$ over 30 cycles, outperforming commercial filters under comparable conditions [113]. These examples illustrate how computationally designed porosity and tailored chemical functionality can extend 3D-printed adsorbents into applications beyond traditional water treatment. Similarly, MOF-based monoliths outperform polymeric scaffolds in gas separation selectivity but show reduced stability in aqueous continuous-flow applications.

In the domain of organic contaminant removal, 3D printing enables the strategic spatial integration of high-affinity materials such as AC, N-doped BC, and functional polymers. These materials contribute multiple adsorption mechanisms, including π–π interactions, hydrogen bonding, and electrostatic effects, within a single monolith. Figure 4 illustrates the selective adsorption mechanism of anionic dyes by the FGA-PC composite. DFT calculations and XPS data reveal that electron transfer occurs from the gelatin-like $(CH_2CONH)_5$ molecule to the graphite-like PC surface, increasing the dipole moment from 4.62 D to 5.10 D and enhancing the positive polarization of functional groups on the composite surface. This charge redistribution facilitates electrostatic attraction toward anionic dyes. Binding energy (BE) simulations indicate stronger interactions between the FGA-PC surface and anionic dyes, with values of -235 kcal mol^{-1} for MO and -312 kcal mol^{-1} for orange G (OG^{2-}), compared to weaker adsorption of cationic dyes such as thiazole yellow (TA^{+}, -151 kcal mol^{-1}) and rhodamine B (RB^{+}, -137 kcal mol^{-1}). Structural modeling further confirms that anionic dyes remain stably anchored to the surface, whereas cationic dyes are more prone to desorption. As illustrated schematically, the material's positively charged surface promotes selective adsorption of anionic species through electrostatic attraction, accounting for its preferential binding behavior.

The growing concern over microplastic contamination in drinking water has prompted interest in 3D-printed filtration systems that offer structural stability and customizable porosity. Scaffolded powdered AC monoliths, reinforced with PEI and fabricated using DIW, have shown effective and selective retention of nanoplastics such as PS, PET, and low-density polyethylene (LDPE) across a range of pH levels and salinity conditions [87]. These structures outperform conventional filters by maintaining mechanical integrity and avoiding particle shedding during extended use, thereby minimizing secondary pollution. As 3D-printed adsorbents frequently involve novel binders, dopants, or nano-scale additives, extensive toxicity and stability assessments are required. Accelerated aging studies, environmental stress testing, and long-term release evaluations must be incorporated early in the development process to satisfy governmental and industry-specific certification protocols.

Table 3. Comparative adsorption performance of 3D-printed adsorbents towards selected adsorbate.

No	Material/printing technique	Pollutant	pH	Mode	Adsorption capacity/efficiency	Selectivity	Reusability	Key Notes	Ref
1	Alginate–gelatin–PEI hydrogel (DIW)	Cu^{2+}, Ni^{2+}, Cd^{2+}, Co^{2+}, Pb^{2+}	4–10	Batch	Cu^{2+}: 633.2 mg g^{-1} (dehydrated); 90.38% at 100 ppm	High ($Cu^{2+} > Ni^{2+} > Cd^{2+}$)	Stable for 240 days	Multilayer adsorption; strong metal affinity	101
2	GO-coated PLA scaffold (FDM)	Cd^{2+}	4–10 (opt. 6)	Batch & Column	1.26 mg g^{-1} (batch); 1.238 mg g^{-1} (column)	—	>90% after 5 cycles	Good mechanical stability in continuous mode	[25]
3	Ca-alginate/GO hydrogel (DIW)	U(VI)	5	Batch	740.74 mg g^{-1} (Ca^{2+}); 847.5 mg g^{-1} (Ca^{2+}+Zn^{2+})	—	97.7% after 9 cycles	Ion-exchange + electrostatic attraction	[105]
4	MIL-101(Cr)/kaolin monolith (DIW)	Butanol, Cyclohexane	– / 40 °C	Continuous (fixed-bed)	215 mg g^{-1} (butanol); 40.4 mg g^{-1} (cyclohexane)	Higher for polar VOCs	—	Bohart-Adams, Clark, and Yan breakthrough models applied	[106]
5	g-C_3N_4/Geopolymer + Fe(III) (DIW)	MB	1–11	Batch (photocatalysis)	92.23% (powder, 30 min); 89.69% (3D-printed, 60 min)	—	<10% loss after 5–10 cycles	Synergistic adsorption + photocatalysis	[105]
6	Polyamide@H_2TiO_3 (PA@HTO) (SLS)	Li^+	12	Batch	1.48 mg g^{-1} (~87% efficiency)	Li/Na ≈ 37.4; Li/K ≈ 60.5	~7% loss after 3 cycles	Endothermic multilayer adsorption; excellent Li^+ selectivity	[107]
7	PPy/ZIF-67/MIL-88A(Fe)/Ti_3CNTx monolith (DLP)	Congo Red (CR), Ag^+	5–7 (CR); 6 (Ag^+)	Batch & Fixed-bed	CR: 1515 mg g^{-1} (batch), 52.61 mg g^{-1} (column); Ag^+: 865 mg g^{-1} (batch), 17 mg g^{-1} (column)	—	Stable for 7 days in water; 30 days in air	Chemisorption (PSO); exothermic adsorption	[108]
8	Cu/Cu_2O-coated PLA scaffold (FDM)	I^-		Batch & Column	4.85 mg g^{-1} (batch);	High versus Cl^-, NO_3^-, SO_4^{2-}; reduced by CO_3^{2-}		Redox-driven CuI formation; stable	[109]

Table 3. (Continued.)

No	Material/printing technique	Pollutant	pH	Mode	Adsorption capacity/efficiency	Selectivity	Reusability	Key Notes	Ref
			3–11 (opt. 3–7)		2.588 mg g^{-1} (column)		Cu leaching <0.08 mg L^{-1} after 24 h	under column flow	
9	GO/SA/PVA dual-network hydrogel (DIW)	Cu^{2+}	1–6 (opt. 5)	Batch & Fixed-bed	206 mg g^{-1} (batch, Langmuir q_{max}); dynamic q_0 = 52.8 mg g^{-1} (Thomas model)	Good $Cu^{2+} > Pb^{2+}$ selectivity	Retains 71.54% capacity after 5 cycles	High compressive strength (≈99 MPa); mesoporous structure; chemisorption mechanism	[110]
10	SiOC/chitosan–GO composite monolith (LCD-SLA)	MO	3	Batch	182.33 mg g^{-1}; 91.16% removal at 50 ppm	—	>92% after 5 cycles	Harkins–Jura isotherm; strong mechanical stability; high BET surface area (78.9 m^2 g^{-1})	[86]
11	FGA–porous carbon composite (DIW)	Orange G, MO	<9 (opt. 3–5)	Batch	99% (OG); 92% (MO) removal after 60 min	Strong preference for anionic dyes versus cationic dyes	—	High BET (1019 m^2 g^{-1}); electron redistribution enhances anionic dye adsorption	[45]
12	DMSA-functionalized GO/cellulose composite (DIW)	Cu^{2+}	5	Batch & Column	~250 mg g^{-1} (batch, 303 K); 51.7–119 mg g^{-1} (dynamic, Thomas model)	—	~80% after 5 cycles	High Cu^{2+} uptake; improved dynamic capacity with bed height	[111]
13	CNT-based sponge (SLA)	Cd^{2+}, Pb^{2+}	NA	Continuous filtration	Cd^{2+}: 40 ± 4% (A); 8 ± 2% (B); Pb^{2+}: 46 ± 4% (A); 84 ± 4% (B)	—	—	Fast uptake in 10 min; validated in tap water; high Pb^{2+} removal selectivity	[112]
14	Carbonaceous porous films (starch-derived carbon + PMMA template, DIW)	Formaldehyde (VOC)	—	Continuous flow	Initial single-pass efficiency: 89%; EACad: 8.6 mg	—	Stable over 30 cycles	Hierarchical porosity (400 nm–100 μm) enabled	[113]

Table 3. (Continued.)

No	Material/printing technique	Pollutant	pH	Mode	Adsorption capacity/efficiency	Selectivity	Reusability	Key Notes	Ref
					g^{-1} (8 h); cumulative EACad: 241.7 mg g^{-1} (30 cycles)			high interfacial diffusion; outperformed commercial filters	
15	Trianglamine hydrogel (SLA, gyroid porous)	PFAS (PFOA, PFOS, PFHpA, PFHxA, PFPeA, PFBS)	~7	Batch	3D-PSHΔ: 92.5% (5 ppm PFOA, 5 h); qmax ≈ 60 mg g^{-1}; 3D-PSHΔQ+: higher uptake & faster kinetics	High PFAS affinity	Retained performance over multiple cycles	Quaternization improved uptake & kinetics; reusable, non-toxic design	[55]

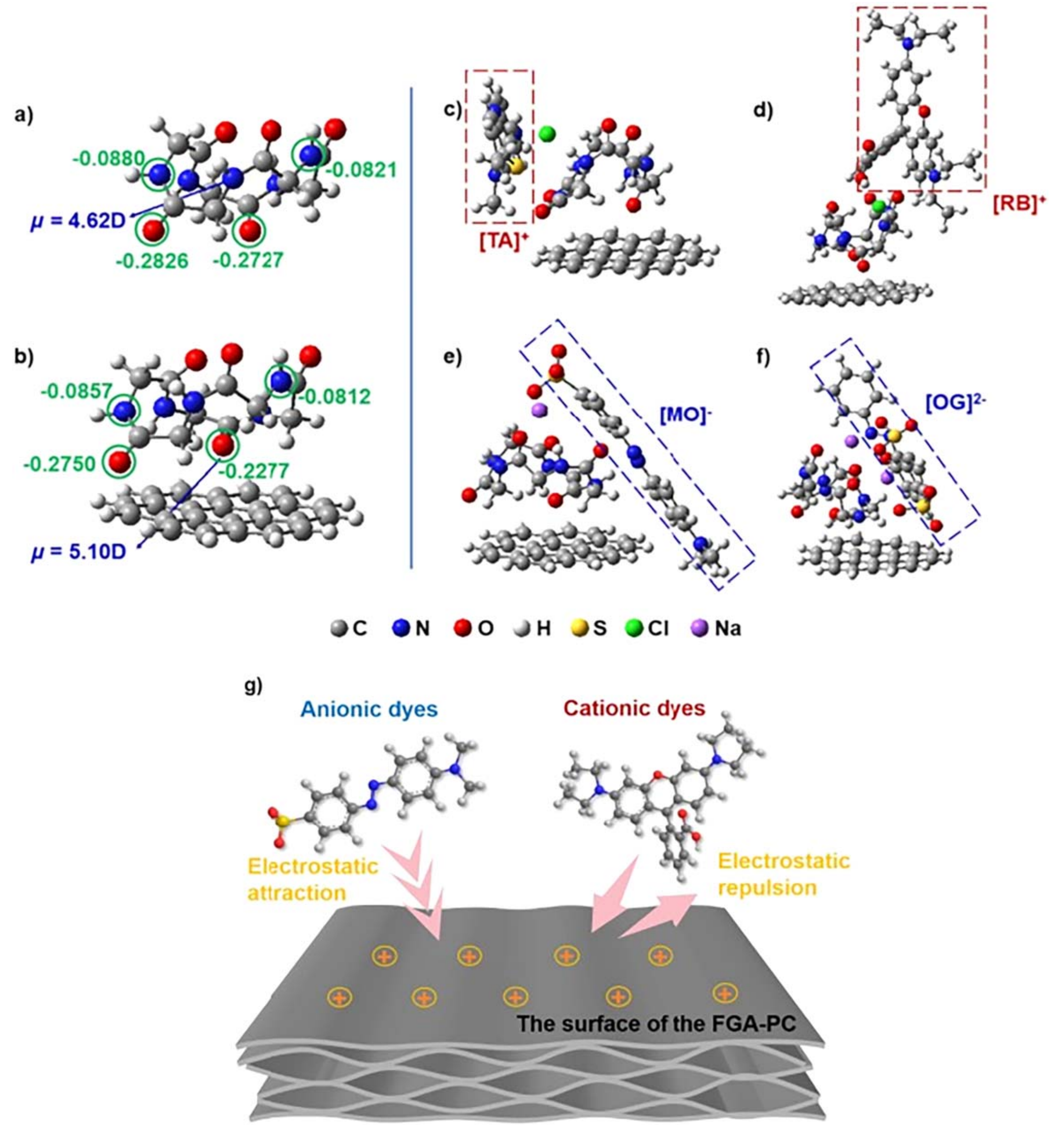

Figure 4. (a) Dipole moment (μ) and Hirshfeld charge values of selected O and N atoms in the simple $(CH_2CONH)_5$; (b) Corresponding μ and Hirshfeld charge values in the $(CH_2CONH)_5$ –coronene composite structure; (c) Simulated interaction between the composite and cationic dye TA^+; (d) Interaction with cationic dye RB^+; (e) Stable binding configuration with anionic dye MO^-; (f) Stable binding configuration with anionic dye OG^{2-}; (g) Schematic representation of the selective adsorption mechanism [45].

6. Challenges, research directions, and outlook

6.1. Current challenges

Despite significant progress, several barriers limit the large-scale adoption of 3D-printed adsorbents for water purification and wastewater treatment. A key issue is the printability of high-performance materials such as MOFs, carbon-based nanostructures, and hybrid bio-inorganic composites. While these materials deliver excellent adsorption capacity and selectivity, their particulate morphology and poor compatibility with printable binders complicate their integration into additive manufacturing workflows. Recent developments, including binder-free CelloZIF-8 [99] and sacrificial templating with $CaCO_3$ [90], are promising, but scalable protocols that preserve functionality are still lacking. Scalability and production throughput also remain critical bottlenecks. Techniques like DIW and SLA provide high structural precision but are inherently slow compared to conventional pellet or monolith fabrication. Industrial translation will require continuous-feed printing, multi-nozzle arrays, and automated post-processing while maintaining the resolution necessary for lattice geometries and pore alignment.

Cost and lifecycle considerations further complicate adoption. Although low-cost renewable inputs such as biochar, geopolymers, and nanocellulose are promising, the capital investment for high-resolution printers, photoinitiators, and thermal post-treatments increases production costs. Comprehensive techno-economic assessments (TEA) and life cycle analyses (LCA) are urgently needed to validate the value proposition of these systems compared to conventional adsorbents. Finally, performance consistency under real-world conditions is underexplored. Many studies focus on static lab-scale testing under controlled pH and ion concentrations, but practical applications involve fluctuating contaminant loads, fouling, and mechanical stress. Reports of MOF scaffold degradation under acidic regeneration and binder leaching during thermal cycling [50] emphasize the need for durable, crosslinked, and pH-tolerant designs validated in dynamic flow environments.

6.2. Future research priorities

Addressing these challenges requires coordinated advancements across several fronts. Developing standardized evaluation protocols for adsorption capacity, selectivity, and regeneration performance under realistic conditions is essential to enable meaningful comparisons between studies and guide material optimization. Comprehensive TEA and LCA are equally critical to quantify the environmental and economic feasibility of 3D-printed adsorbents, including potential benefits such as reduced waste generation, lower regeneration energy requirements, and modular reuse. Clear regulatory frameworks must also be established to address material safety, leaching behavior, recyclability, and certification, ensuring compliance for industrial and municipal applications.

However, these limitations also present opportunities for innovation. The integration of computational modeling and AI-assisted design enables predictive engineering of adsorbent geometries tailored for specific fluid dynamics and contaminant profiles [114, 115]. Techniques such as topology optimization, CFD, and FEA offer a pre-fabrication filter to eliminate inefficient designs and reduce empirical iteration. Similarly, machine learning models can predict pH-dependent adsorption kinetics and guide ink formulation or structural adjustments, effectively bridging materials informatics with digital manufacturing. Furthermore, functionally graded and multi-material printing enables the fabrication of spatially heterogeneous structures. These adsorbents can incorporate hydrophilic and hydrophobic domains, acidic and basic functional groups, or sequential zones for adsorption and catalysis. Such designs provide a pathway toward customizable treatment systems capable of addressing multicomponent pollutant mixtures and facilitating *in situ* regeneration without the need for disassembly.

The convergence of bioinspired geometries, such as gyroid or vascular networks, with algorithmically generated structures may soon define a new class of intelligent, flow-adaptive adsorbents. From a sustainability perspective, the incorporation of industrial waste valorization strategies into printable feedstocks can reduce ecological impact while creating cost-effective, circular materials for remediation [116–119]. When paired with renewable-powered printing systems, this represents a blueprint for green additive manufacturing in environmental technologies. Furthermore, multi-material and functionally graded printing approaches warrant deeper investigation, as they can improve interfacial bonding and enable the creation of hybrid structures with synergistic properties for multi-contaminant treatment and integrated catalytic or sensing functions.

6.3. Outlook

3D-printed adsorbents represent a paradigm shift in water treatment technology, offering unmatched design flexibility, modularity, and application-specific functionality. Advancing toward full-scale deployment will depend on harmonizing material innovation, scalable manufacturing, computational design, and regulatory readiness. By addressing these priorities, the next generation of 3D-printed adsorbents can achieve functional precision, sustainable production, and predictive adaptability, positioning additive manufacturing as a cornerstone for advanced environmental remediation solutions.

In conclusion, the future of 3D-printed adsorbents will be shaped by how effectively emerging materials, manufacturing innovations, and computational tools are integrated to deliver scalable, compliant, and high-performance systems. Beyond enhancing individual metrics, success will depend on full-system integration, cost-effectiveness, and regulatory alignment. As additive manufacturing technologies continue to mature, the next generation of adsorbents will likely embody the principles of functional precision, sustainable design, and predictive adaptability, driving their transition from laboratory concepts to robust industrial and municipal treatment solutions.

Compliance with ethical standards

This study did not involve any live experimentation on human participants or animals. All analyses were based on secondary data, published literature, or computational/analytical methods. Ethical approval was therefore not required.

Competing interest

The authors declare that they have no known competing financial interests or personal relationships that could have appeared to influence the work reported in this paper.

Ethics approval

Not applicable.

Consent to participate

Not applicable.

Consent for publication

All authors reviewed and agreed to the final manuscript for publication.

Fundings

This work was supported by Universiti Putra Malaysia Grant GP-IPM/9750400. The authors confirm that there are no additional funders. The funder had no role in study design, data collection and analysis, decision to publish, or preparation of the manuscript. The authors acknowledged the anonymous reviewers for comments to improve the quality of this work.

Data availability statement

All data that support the findings of this study are included within the article (and any supplementary files).

Author contributions

Alvin Lim Teik Zheng 0000-0001-5071-0156
Conceptualization (lead), Funding acquisition (lead), Methodology (lead), Software (lead), Writing – original draft (equal)

Ellie Yi Lih Teo 0000-0001-8212-9788
Validation (lead), Writing – original draft (supporting)

Omar Faruqi Marzuki 0000-0002-7134-7277
Software (lead), Visualization (lead)

Lee Feng Koo 0000-0002-9957-9571
Methodology (supporting), Writing – original draft (supporting)

Tze Jin Wong 0000-0003-2004-0088
Funding acquisition (supporting), Methodology (supporting), Software (supporting)

Eric Lim Teik Chung 0000-0003-1038-1057
Conceptualization (supporting), Methodology (supporting), Writing – original draft (equal), Writing – review & editing (equal)

Yoshito Andou 0000-0003-3839-0705
Conceptualization (equal), Supervision (lead), Writing – original draft (equal), Writing – review & editing (equal)

References

[1] Chew T W, H'Ng P S, Luqman Chuah Abdullah B C T G, Chin K L, Lee C L, Mohd Nor Hafizuddin B M S and TaungMai L 2023 A review of bio-based activated carbon properties produced from different activating chemicals during chemicals activation process on biomass and its potential for Malaysia *Materials* **16** 7365

[2] Husien S, El-taweel R M, Salim A I, Fahim I S, Said L A and Radwan A G 2022 Review of activated carbon adsorbent material for textile dyes removal: preparation, and modelling *Current Research in Green and Sustainable Chemistry* **5** 100325

[3] Azam K, Shezad N, Shafiq I, Akhter P, Akhtar F, Jamil F, Shafique S, Park Y-K and Hussain M 2022 A review on activated carbon modifications for the treatment of wastewater containing anionic dyes *Chemosphere* **306** 135566

[4] Zheng A L T, Teo E Y L, Yiu P H, Boonyuen S, Chung E L T and Andou Y 2025 Recent advances in ultrasensitive electrochemical sensors and biosensors for determination of antibiotics in environment samples *Clean Technol. Environ. Policy* **27** 549–76

[5] Kumar A, Dutt S, Kumar R and Sonika 2023 Use of 3D printed techniques for organic pollutants removal *3D Printing Technology for Water Treatment Applications* (Elsevier) 193–211

[6] Comroe M L, Kolasinski K W and Saha D 2022 Direct Ink 3D printing of porous carbon monoliths for gas separations *Molecules* **27** 5653

[7] Jivrakh K B, Kuppireddy S, Dumée L F, Polychronopoulou K, Abu Al-Rub R K, Alamoodi N and Karanikolos G N 2024 A critical review on 3D-printed adsorbents, membranes, and catalysts for carbon dioxide capture, separation, and conversion *J. Clean. Prod.* **472** 143522

[8] Yu J, Zhu J, Chen L, Chao Y, Zhu W and Liu Z 2023 A review of adsorption materials and their application of 3D printing technology in the separation process *Chem. Eng. J.* **475** 146247

[9] Lawson S, Li X, Thakkar H, Rownaghi A A and Rezaei F 2021 Recent advances in 3D Printing of structured materials for adsorption and catalysis applications *Chem. Rev.* **121** 6246–91

[10] Finny A S 2024 3D bioprinting in bioremediation: a comprehensive review of principles, applications, and future directions *PeerJ* **12** e16897

[11] Soliman A, AlAmoodi N, Karanikolos G N, Doumanidis C C and Polychronopoulou K 2020 A review on new 3-D printed materials' geometries for catalysis and adsorption: paradigms from reforming reactions and CO2 capture *Nanomaterials* **10** 2198

[12] Roy Barman S, Gavit P, Chowdhury S, Chatterjee K and Nain A 2023 3D-printed materials for wastewater treatment *JACS. Au.* **3** 2930–47

[13] Asghartabar Kashi P, Mohammadi A, Chen J, Ettelaie R, Jäger H and Shahbazi M 2024 3D printing of a photo-curable hydrogel to engineer mechanically robust porous structure for ion capture or sustained potassium ferrate(VI) release for water treatment *Sep. Purif. Technol.* **344** 127247

[14] Lee J, Chuah C Y, Tan W S, Song J and Bae T-H 2022 3D-printed monolithic porous adsorbents from a solution-processible, hypercrosslinkable, functionalizable polymer *Chem. Eng. J.* **427** 130883

[15] Penumakala P K, Santo J and Thomas A 2020 A critical review on the fused deposition modeling of thermoplastic polymer composites *Composites* B **201** 108336

[16] Hu C and Qin Q-H 2020 Advances in fused deposition modeling of discontinuous fiber/polymer composites *Curr. Opin. Solid State Mater. Sci.* **24** 100867

[17] Özen A and Auhl D 2022 Modeling of the mechanical properties of fused deposition modeling (FDM) printed fiber reinforced thermoplastic composites by asymptotic homogenization *Composites and Advanced Materials* **31**

[18] Saadi M A S R, Maguire A, Pottackal N T, Thakur M S H, Ikram M M, Hart A J, Ajayan P M and Rahman M M 2022 Direct ink writing: a 3D printing technology for diverse materials *Adv. Mater.* **34**

[19] Chen B, Jiang Q, Tu J, Xiong X and Cui J 2025 Direct ink writing additive manufacturing of silica aerogels *Chem. Sus. Chem.* **18**

[20] Castro J, Nóbrega J M and Costa R 2024 Computational framework to model the selective laser sintering process *Materials* **17** 1845

[21] Yehia H M, Hamada A, Sebaey T A and Abd-Elaziem W 2024 Selective laser sintering of polymers: process parameters, machine learning approaches, and future directions *Journal of Manufacturing and Materials Processing* **8** 197

[22] Tang J, Guo X, Chang H, Hu K, Shen Z, Wang W, Liu M, Wei Y, Huang Z and Yang Y 2021 The preparation of SiC ceramic photosensitive slurry for rapid stereolithography *J. Eur. Ceram. Soc.* **41** 7516–24

[23] Karatza A, Zouboulis P, Gavalas I, Semitekolos D, Kontiza A, Karamitrou M, Koumoulos E P and Charitidis C 2022 SLA resins modification by liquid mixing with ceramic powders aiming at mechanical property and thermal stability enhancement for rapid tooling applications *Journal of Manufacturing and Materials Processing* **6** 129

[24] Wu L and Song Y 2025 Recent innovations in interfacial strategies for DLP 3D printing process optimization *Mater Horiz* **12** 401–17

[25] Park S-S, Park Y, Repo E, Shin H-S and Hwang Y 2024 Three-dimensionally printed scaffold coated with graphene oxide for enhanced heavy metal adsorption: Batch and fixed-bed column studies *Journal of Water Process Engineering* **57** 104658

[26] Scott S, Chew J, Barnard J, Burrows A, Smith M, Tennison S and Perera S 2023 Tailoring 3D printed micro-structured carbons for adsorption *Adv. Funct. Mater.* **33** 22137715

[27] Grigor E, Carver J, Bulan E, Scott S, Chew Y J and Perera S 2024 A new generation of activated carbon adsorbent microstructures *Adv. Sci.* **11**

[28] Han W, Kong L and Xu M 2022 Advances in selective laser sintering of polymers *International Journal of Extreme Manufacturing* **4** 042002

[29] Joralmon D, Tang T, Jayant L, Yoo M and Li X 2024 Recent advances and prospects in selective laser sintering (SLS) and melting (SLM) and multiphoton lithography for 3D printing *laser-based Techniques for Nanomaterials* (Royal Society of Chemistry) 185–217

[30] Sun P, Zhang L and Tao S 2019 Preparation of hybrid chitosan membranes by selective laser sintering for adsorption and catalysis *Mater. Des.* **173** 107780

[31] Weiss J D *et al* 2025 A low-cost, open-source 3D printer for multimaterial and high-throughput direct ink writing of soft and living materials *Adv. Mater.* **37** 2414971

[32] Geng P and Jiang C 2025 Direct ink writing 3D printing polytetrafluoroethylene/polydimethylsiloxane membrane with anisotropic surface wettability and its application in oil–water separation *Polymers* **17** 174

[33] Maier A S, Lackner F, Fink J, Steindorfer T, Hofmann E, Stana Kleinschek K and Rieger B 2025 High-fidelity direct ink writing of poly (vinylphosphonate)-reinforced polysaccharide inks with tunable properties *ACS. Appl. Polym Mater* **7** 1752–62

[34] Valenzuela C, Ma S, Yang Y, Chen Y, Zhang X, Wang L and Feng W 2025 Direct ink writing of 3D chiral soft photonic crystals *Adv. Funct. Mater.* (https://doi.org/10.1002/adfm.202421280)

[35] Pradal P, Kim J B, Nam S K, Kim S and Amstad E 2025 Direct ink writing of rigid microparticles *Small* **21** 2405675

[36] Liu Z, Zhou X and Liu C 2019 N-doped porous carbon material prepared via direct ink writing for the removal of methylene blue *Diam. Relat. Mater.* **95** 121–6
[37] Alison L, Menasce S, Bouville F, Tervoort E, Mattich I, Ofner A and Studart A R 2019 3D printing of sacrificial templates into hierarchical porous materials *Sci. Rep.* **9** 409
[38] Xie L *et al* 2024 Balanced mass transfer and active sites density in hierarchical porous catalytic metal–organic framework for enhancing redox reaction in lithium–sulfur batteries *ACS. Nano* **18** 12820–9
[39] Xiao Y-Y, Liu X-L, Chang G-G, Pu C, Tian G, Wang L-Y, Liu J-W, Ma X-C, Yang X-Y and Chen B 2020 Construction of a functionalized hierarchical pore metal–organic framework via a palladium-reduction induced strategy *Nanoscale* **12** 6250–5
[40] Chisăliţă D-A, Boon J and Lücking L 2025 Adsorbent shaping as enabler for intensified pressure swing adsorption (PSA): a critical review *Sep. Purif. Technol.* **353** 128466
[41] Wang D, Zhi T, Liu L, Yan L, Yan W, Tang Y, He B, Hu L, Jing C and Jiang G 2022 3D printing of TiO2 nano particles containing macrostructures for As(III) removal in water *Sci. Total Environ.* **815** 152754
[42] Lin H, Shen Q, Ma M, Ji R, Guo H, Qi H, Xing W and Tang H 2025 3D Printing of porous ceramics for enhanced thermal insulation properties *Adv. Sci.* **12** 2412554
[43] Lee J-C, Kim D-Y, Lee E-H and Lee S-W 2024 Empowering powdered activated carbon (PAC) with 3D printing: achieving highly efficient and reusable cationic dye removal *Chemosphere* **357** 141982
[44] Liu X *et al* 2023 Advanced porous nanomaterials as superior adsorbents for environmental pollutants removal from aqueous solutions *Crit Rev Environ Sci Technol* **53** 1289–309
[45] Li J-X, Zhao Y-J, Yu Y-F, Huang Q-Q, Qi S-C, Liu X-Q and Sun L-B 2025 The selective adsorption of anionic dyes over 3D printing composite sorbents of aerogel and porous carbon *Sep. Purif. Technol.* **360** 130945
[46] Abubakar A J A, Canevesi R L S, Sanchez D A L and Grande C A 2024 Monoliths for gas storage manufactured with precision pore engineering using 3D-printed templates *Chem. Eng. J.* **489** 151450
[47] Zhu J, Yu J, Wu P, Liu J, Ji H, Huang Y, Chao Y, Liu H, Zhu W and Liu Z 2024 3D printing of hierarchically porous lightweight activated carbon/alumina monolithic adsorbent for adsorptive desulfurization of hydrogenated diesel *Sep. Purif. Technol.* **330** 125334
[48] Nia N D, Kim B, Park Y, Yun Y-M, Repo E and Hwang Y 2025 Layer-by-layer synthesis of copper hexacyanoferrate on 3D-printed scaffolds for efficient ammonium recovery *Water Res. X.* **28** 100322
[49] Wu T, Karimi-Maleh H, Li Y, Zhang Z, Zhang D, Wen Y, Fu L, Zhong N, Dragoi E N and Aminabhavi T M 2024 3D printed monolithic nanocomposites as adsorbents to remove Congo red and mercury (II) from wastewater *Chem. Eng. J.* **501** 157710
[50] Bauzà M, Figuerola A, Turnes Palomino G and Palomino Cabello C 2025 ZIF-8 derived carbon@3D-printed columns as efficient continuous-flow adsorbents of parabens from water *J. Hazard. Mater.* **484** 136697
[51] Charalampous P, Pelekoudas A, Kostavelis I, Ioannidis D and Tzovaras D 2024 An integrated modeling framework for automated product design, topology optimization, and mechanical simulation *Journal of Manufacturing and Materials Processing* **8** 285
[52] Jin H, Hong K, Liu J, Qiu C, Zhu M, Li C and Wang Q 2025 Structural and functional design of CTAB-geopolymer adsorbents for rapid removal of tetracycline: a comparative study *Sep. Purif. Technol.* **356** 129872
[53] Mohd Yusoff N H, Irene Teo L-R, Phang S J, Wong V-L, Cheah K H and Lim S-S 2022 Recent advances in polymer-based 3D printing for wastewater treatment application: an overview *Chem. Eng. J.* **429** 132311
[54] Shahzadi L, Maya F, Breadmore M C and Thickett S C 2023 Thiol-yne 3D printable polymeric resins for the efficient removal of a model pollutant from waters *Macromol. Mater. Eng.* **308** 2200497
[55] Chaix A *et al* 2025 Efficient PFAS removal using reusable and non-toxic 3D printed porous trianglamine hydrogels *Adv. Mater.* **37** 2410720
[56] Della Rocca D G, Peralta R M, Peralta R A, Rodríguez-Castellón E and de Fatima Peralta Muniz Moreira R 2021 Adding value to aluminosilicate solid wastes to produce adsorbents, catalysts and filtration membranes for water and wastewater treatment *J. Mater. Sci.* **56** 1039–63
[57] El Alouani M, Aouan B, Rachdi Y, Alehyen S, El Herradi E H, Saufi H, Mabrouki J and Barka N 2024 Porous geopolymers as innovative adsorbents for the removal of organic and inorganic hazardous substances: a mini-review *Int. J. Environ. Anal. Chem.* **104** 4784–96
[58] Adewuyi Y G 2021 Recent advances in fly-ash-based geopolymers: potential on the utilization for sustainable environmental remediation *ACS. Omega* **6** 15532–42
[59] Sandanamsamy L, Mogan J, Halim N A, Harun W S W, Kadirgama K and Ramasamy D 2021 A review on 3D printing bio-based polymer composite *IOP Conf. Ser.: Mater. Sci. Eng.* **1078** 012031
[60] Shahbazi M and Jäger H 2021 Current status in the utilization of biobased polymers for 3D printing process: a systematic review of the materials, processes, and challenges *ACS. Appl. Bio. Mater* **4** 325–69
[61] Wang Q, Sun J, Yao Q, Ji C, Liu J and Zhu Q 2018 3D printing with cellulose materials *Cellulose* **25** 4275–301
[62] Gauss C, Pickering K L and Muthe L P 2021 The use of cellulose in bio-derived formulations for 3D/4D printing: a review *Composites C* **4** 100113
[63] Zhou L, Ramezani H, Sun M, Xie M, Nie J, Lv S, Cai J, Fu J and He Y 2020 3D printing of high-strength chitosan hydrogel scaffolds without any organic solvents *Biomater. Sci.* **8** 5020–8
[64] Sahranavard M, Zamanian A, Ghorbani F and Shahrezaee M H 2020 A critical review on three dimensional-printed chitosan hydrogels for development of tissue engineering *Bioprinting* **17** e00063
[65] Ahmadi Soufivand A, Faber J, Hinrichsen J and Budday S 2023 Multilayer 3D bioprinting and complex mechanical properties of alginate-gelatin mesostructures *Sci. Rep.* **13** 11253
[66] Stavarache C, Gârea S A, Serafim A, Olăreţ E, Vlăsceanu G M, Marin M M and Iovu H 2024 Three-dimensional-printed sodium alginate and k-carrageenan-based scaffolds with potential biomedical applications *Polymers* **16** 305
[67] Mallakpour S, Azadi E and Hussain C M 2021 State-of-the-art of 3D printing technology of alginate-based hydrogels—An emerging technique for industrial applications *Adv. Colloid Interface Sci.* **293** 102436
[68] N'Gatta K M, Belaid H, El Hayek J, Assanvo E F, Kajdan M, Masquelez N, Boa D, Cavaillès V, Bechelany M and Salameh C 2022 3D printing of cellulose nanocrystals based composites to build robust biomimetic scaffolds for bone tissue engineering *Sci. Rep.* **12** 21244
[69] Sajab M S, Wan Jusoh W N L, Mohan D, Kaco H and Baini R 2023 3D printed functionalized nanocellulose as an adsorbent in batch and fixed-bed systems *Polymers* **15** 969
[70] Rianjanu A, Taher T, Desriani F, Delmita R O, Sianturi A G N, Muhtar S A, Ariwahjoedi B, Khamidy N I, Adhika D R and Arif M F 2024 Examining the influence of sintering temperatures on the efficiency of 3D-printed natural zeolite for methylene blue dye adsorption *Results in Surfaces and Interfaces* **17** 100337

[71] Khalil A, Hashaikeh R and Hilal N 2021 3D printed zeolite-Y for removing heavy metals from water *Journal of Water Process Engineering* **42** 102187
[72] Kennedy A J, Ballentine M L, May L R, Das A, Bednar A J, Griggs C S, Hull M S and Bortner M J 2022 Simplifying complex contaminant mixtures: selective ammonia adsorption and toxicity reduction using 3D printable polymer–zeolite *Water Air Soil Pollut.* **233** 148
[73] Aldoghachi A, Yun Hin T-Y, Saiman M I, Voon L H, Zheng A L T and Seenivasagam S 2024 Development of highly stable Ni-doped zeolitic imidazole framework (ZIF-67) based catalyst for CO2 methanation reaction *Int. J. Hydrogen Energy* **57** 1474–85
[74] Zheng A L T, Teo E Y L, Seenivasagam S, Yiu P H, Boonyuen S, Chung E L T and Andou Y 2024 Recent review on porous adsorbents for water decontamination: strategies for enhanced removal of tetracycline *J. Porous Mater.* **32** 1–25
[75] Zheng A L T, Teo E Y L, Seenivasagam S, Yiu P H, Boonyuen S, Chung E L T, Lease J and Andou Y 2024 Nanostructures embedded on porous materials for the catalytic reduction of nitrophenols: a concise review *J. Porous Mater.* **31** 1557–75
[76] Molavi H, Mirzaei K, Barjasteh M, Rahnamaee S Y, Saeedi S, Hassanpouryouzband A and Rezakazemi M 2024 3D-printed MOF monoliths: fabrication strategies and environmental applications *Nanomicro Lett* **16** 272
[77] Zou D, Liu D and Zhang J 2018 From zeolitic imidazolate framework-8 to metal-organic frameworks (MOFs): representative substance for the general study of pioneering MOF applications *Energy & Environmental Materials* **1** 209–20
[78] Crespí Sánchez N, Turnes Palomino G and Palomino Cabello C 2023 Sulfonic-functionalized MIL-100-Fe MOF for the removal of diclofenac from water *Microporous Mesoporous Mater.* **348** 112398
[79] Zheng A L T and Andou Y 2022 Hybrid three-dimensional (3D) graphene architectures for photocatalysis of noxious pollutants *Green Nanoarchitectonics* (Jenny Stanford Publishing) 47–72
[80] Zheng A L T, Boonyuen S, Ohno T and Andou Y 2021 Hydrothermally reduced graphene hydrogel intercalated with divalent ions for dye adsorption studies *Processes* **9** 169
[81] Zheng A L T, Ohno T and Andou Y 2022 Recent progress in photocatalytic efficiency of hybrid three-dimensional (3D) graphene architectures for pollution remediation *Top. Catal.* **65** 1634–47
[82] Zheng A L T, Che Abdullah C A and Andou Y 2023 Graphene-based nanomaterials for water remediation applications *Handbook of Green and Sustainable Nanotechnology* (Springer International Publishing) 1097–122
[83] Wu Y, An C and Guo Y 2023 3D printed graphene and graphene/polymer composites for multifunctional applications *Materials* **16** 5681
[84] Wu X, Mu F and Lin Z 2021 Three-dimensional printing of graphene-based materials and the application in energy storage *Mater Today Adv* **11** 100157
[85] Zheng A L T, Boonyuen S, Li G Y, Ngee L H and Andou Y 2021 Design of reduced graphene hydrogel with alkylamine surface functionalization through immersion/agitation method and its adsorption mechanism *J. Mol. Struct.* **1245** 131008
[86] Xin Yong G T, Koh W B, Binti Mohd Yusoff N H, Norman A, Chong C H, Cheah K H and Wong V-L 2025 3D-printed SiOC ceramics grafted with chitosan-graphene oxide composite for enhanced dye adsorption *Sep. Purif. Technol.* **362** 131669
[87] Kim N, Kim D-Y, Chang Y, Jung E-M, Lee S-W and Lee E-H 2025 Addressing plastic pollution: a 3D-printed porous PAC scaffold for effective nanoplastic removal *Chemosphere* **377** 144351
[88] Mian M M and Liu G 2018 Recent progress in biochar-supported photocatalysts: synthesis, role of biochar, and applications *RSC Adv.* **8** 14237–48
[89] Zheng A L T, Lih E T Y, Hung Y P, Boonyuen S, Al Edrus S S O, Chung E L T and Andou Y 2025 Biochar-based electrochemical sensors: a tailored approach to environmental monitoring *Anal. Sci.* **41** 715–35
[90] Zhou Z, Xu K, Li C, Lin J, Bian J, Sun K, Jiang J, Zhou S-F and Zhan G 2024 Assembly of 3D printed N-doped biochar as impeller with CaCO3 as sacrificial pore generator for enhanced dye adsorption *Chem. Eng. J.* **497** 154661
[91] Iqbal Z, Tanweer M S and Alam M 2022 Recent advances in adsorptive removal of wastewater pollutants by chemically modified metal oxides: a review *Journal of Water Process Engineering* **46** 102641
[92] Yang Y, Hao X, Sun Z, Chen Y, Xu Z and Zhao W 2024 Fabrication of metal oxides-based adsorbents for SO2 capture with equimolar adsorption *Chem. Eng. J.* **486** 150106
[93] Maran M A, Zheng A L T, Tan H Y, Sarbini S R, Tan K B, Boonyuen S, Wong K K S, Chung E L T, Lease J and Andou Y 2025 Assessing the photocatalytic performance of hydrothermally synthesized Fe-doped BiVO4 under low-intensity UV irradiation *Arab. J. Sci. Eng.* (https://doi.org/10.1007/s13369-025-10278-8)
[94] Tirado-González J G, Esguerra-Arce J, Esguerra-Arce A and Herrera-Quintero L K 2024 3D printing iron/iron oxide composites by metal material extrusion from an industrial waste *JOM* **76** 1924–36
[95] Martins A S, Zoumpouli G A, Yi S, Exposito A J, Wenk J and Mattia D 2024 3D-printed indium oxide monoliths for PFAS removal *Chem. Eng. J.* **497** 154366
[96] Wang L, Shi C, Wang L, Pan L, Zhang X and Zou J-J 2020 Rational design, synthesis, adsorption principles and applications of metal oxide adsorbents: a review *Nanoscale* **12** 4790–815
[97] Meena P L and Surela A K 2024 Carbon-polyaniline composite adsorbents for aqueous pollutants uptake *Reference Module in Materials Science and Materials Engineering* (Elsevier) (https://doi.org/10.1016/B978-0-323-95486-0.00003-X)
[98] Far H S, Najafi M, Hasanzadeh M and Rahimi R 2022 A 3D-printed hierarchical porous architecture of MOF@clay composite for rapid and highly efficient dye scavenging *New J. Chem.* **46** 23351–60
[99] Nasser Abdelhamid H, Sultan S and Mathew A P 2023 Binder-free three-dimensional (3D) printing of cellulose-ZIF8 (CelloZIF-8) for water treatment and carbon dioxide (CO_2) adsorption *Chem. Eng. J.* **468** 143567
[100] Scaffaro R, Mistretta M C and Balsamo M 2024 Innovative 3D-printed devices for water pollutant removal: comprehensive review on printing parameters, composition, properties and performances of the latest 3D-systems *Polym. Test.* **140** 108627
[101] Finny A S, Cheng N, Popoola O and Andreescu S 2022 3D printable polyethyleneimine based hydrogel adsorbents for heavy metal ions removal *Environmental Science: Advances* **1** 443–55
[102] Rozyyev V, Gao F, Liu Y, Shevate R, Pathak R, Mane A U, Darling S B and Elam J W 2024 Thiol-functionalized adsorbents through atomic layer deposition and vapor-phase silanization for heavy metal ion removal *ACS Appl. Mater. Interfaces* **16** 34030–41
[103] Zhou Y, Xiong J, Wang L, Li F, Bai H, Wang S and Yang X 2024 Multi-ligand strategy for enhanced removal of heavy metal ions by thiol-functionalized defective Zr-MOFs *J. Hazard. Mater.* **479** 135723
[104] Yang J, Lin Y, Wang X, Li Y, Deng Y and Zheng C 2024 3D printed microplasma optical emission spectrometry coupled with ZIF-8 based dispersive solid-phase extraction for field analysis of waterborne arsenic *Anal. Chim. Acta* **1330** 343270
[105] Liu X, Zhao S, Li Q, He P, Duan X, Jia D, Colombo P and Zhou Y 2025 Enhancing methylene blue removal performance through interfacial charge transfer effect in 3D printing g-C3N4/geopolymer/Fe(Ⅲ) composite *J. Environ. Chem. Eng.* **13** 117846

[106] Rico-Barragán A A, Ávila-Lopéz M A, Cruz J B, Lara-Ceniceros T E, Rojas Mayorga C K, Aguayo-Villarreal I A, Ibarra I A, Lalinia M, Moreno-Pérez J and Dávila-Guzmán N E 2025 3D-printed MIL-101(Cr)-monoliths for butanol and cyclohexane removal: insights into rheological behavior and adsorption capacity *Mater. Sci. Eng.* B **320** 118449

[107] Bandina E, Elkabous M, Iurchenkova A, Ouardi Y E and Repo E 2025 3D-printed polyamide-H2TiO3 composite for selective lithium adsorption: insights from experimental and theoretical dynamic simulations studies *Miner. Eng.* **231** 109470

[108] Wu T, Zare N, Li Y, Zhang D, Dragoi E N, Aminabhavi T M and Karimi-Maleh H 2025 3D printed monolithic adsorbent for removal of congo red and silver ions: batch and fixed bed column studies *Chem. Eng. J.* **519** 164865

[109] Kim B, Park Y, Kim H-W, Kim J-A and Hwang Y 2025 Enhanced iodide removal from aqueous solutions using 3D-printed PLA scaffold coated with Cu/Cu_2O nanoparticles *Environ. Res.* **279** 121835

[110] Zhang H, Shi Z, Liu X, Wang B, Niu W, Cai W, Wu Z, Zhu Y, Guo Q and Wang H 2025 Insights into graphene oxide double-network macro-monothlic adsorbent through 3D printing: mechanical properties and Cu2+ adsorption mechanism *Sep. Purif. Technol.* **363** 132140

[111] Colozza N, Arduini F, Duranti L, Limosani F, Rosati M, Amendola L and Scarselli M 2025 3D Sponge-like structures of carbon nanotubes for heavy metal adsorption *ACS Appl. Nano Mater.* **8** 13199–212

[112] Zhang H, Shi Z, Wang B, Han J, Liu X, Zhao Y and Niu W 2025 Hierarchical 3D architectured DMSA-functionalized SA/GO-cellulose monoliths via direct ink writing: enhanced Cu^{2+} removal and synergistic adsorption mechanisms *J. Polym. Environ.* **33** 2721–38

[113] Chen Z, Chen Q, Wang Y, Zou W, Li Y and Mo J 2025 Tuning multi-scale pore structures in carbonaceous films via direct ink writing and sacrificial templates for efficient indoor formaldehyde removal *J. Hazard. Mater.* **487** 137203

[114] Zhao Z, Baumann A and Ryan E M 2024 Using machine-learning-aided computational fluid dynamics to facilitate design of experiments *Ind. Eng. Chem. Res.* **63** 21444–54

[115] Pellegrini J and Celis J de 2024 Refinement of a kinetic adsorption model through artificial intelligence *Brazilian Journal of Development* **10** e75662

[116] Rossi D, Lermen F H and Echeveste M E 2025 Circular product development strategies for sustainable production and consumption based on waste valorization *Management of Environmental Quality: An International Journal* **36** 470–90

[117] Al Rashid A and Koç M 2024 Economically viable plastic recycling to produce additive manufacturing feedstock using waste bottles for circular economy *Advanced Manufacturing* vol 2 (American Society of Mechanical Engineers) (https://doi.org/10.1115/IMECE2024-140719)

[118] Toghan A, Alduaij O K, Sanad M M S and Elessawy N A 2024 Scalable engineering of 3D printing filaments derived from recycling of plastic drinking water bottle and glass waste *Polymers* **16** 3195

[119] Peter R N A, Zheng A L T, Koo L F, Wong T J and Andou Y 2025 Upcycling mine tailings into functional materials for environmental remediation and energy storage applications *International Journal of Energy and Water Resources* (https://doi.org/10.1007/s42108-025-00391-7)

[120] Bahmanzadegan F and Ghaemi A 2025 A comprehensive review on novel zeolite-based adsorbents for environmental pollutant *Journal of Hazardous Materials Advances* **17** 100617

[121] Sowa M, Sztekler K, Mlonka-Mędrala A and Mika Ł 2023 An Overview of Developments In Silica Gel Matrix Composite Sorbents for Adsorption Chillers with Desalination Function *Energies* **16** 5808

[122] Rasheed T, Hassan A A, Bilal M, Hussain T and Rizwan K 2020 Metal-organic frameworks based adsorbents: A review from removal perspective of various environmental contaminants from wastewater *Chemosphere* **259** 127369

[123] Zhu G, Hou Y, Xu J and Zhao N 2022 Digital Light Processing 3D Printing of Enhanced Polymers via Interlayer Welding *Macromolecular Rapid Communications* **43** 2200053